

17th CIRP Conference on Modelling of Machining Operations

## Modelling the dynamics of a large damped boring bar in a lathe.

Dan Östling<sup>a\*</sup>, Martin Magnevall<sup>b</sup>

<sup>a</sup>Sandvik Coromant Trondheim, Ranheimsveien 127, 7053 Ranheim, Norway

<sup>b</sup>Sandvik Coromant, Mossvägen, Sandviken, Sweden

<sup>b</sup>Blekinge Institute of Technology, Karlskrona, Sweden

\* Corresponding author. Tel.: +47-90920498. E-mail address: [dan.ostling@sandvik.com](mailto:dan.ostling@sandvik.com)

### Abstract

Boring bars with tuned mass dampers have a passive damper tuned with respect to the frequency of the first bending mode of the tool. When the tool is clamped into the machine tool there is a stiffness loss that lowers the natural frequency of the bar compared to ideal clamping conditions. For large tools the difference can be more than 35%, depending on clamping structure, tool size and overhang. In this paper we investigate a simple two-degree-of-freedom model for the tool-machine interaction consisting of a bending mode coupled with a rotational stiff mode. The model gives good insight into the system behavior and fits well with measurements.

© 2019 The Authors. Published by Elsevier B.V.

Peer-review under responsibility of the scientific committee of The 17th CIRP Conference on Modelling of Machining Operations

*Keywords:* Internal turning; tuned mass damper; tool clamping

### 1. Background

Boring bars with tuned mass dampers (TMD) have proved very successful in suppressing chatter in various internal turning operations. The damper increases process stability and allows for stable machining with slender tools in deep holes [1]. The especially big boring bars we are addressing in this paper are typically used for various forged hydraulic cylinders and tubes for the oil and gas industry. Here the turning tool can become large and heavy compared to the machine-tool clamping and the whole system must be considered in the design of the damped tool. The largest bar delivered to date weighs 6000kg, has a diameter  $D=500\text{mm}$  and is clamped at an overhang of 5m in a big flatbed lathe.

When designing a damped boring bar, the main challenge is to find the right tuning of the TMD with respect to the vibration frequency of the bar, usually the natural frequency of the first bending mode. The frequency of the bar itself can be easily

found from the CAD files by an eigenfrequency simulation in an FE program like ANSYS.

The optimal damper frequency will depend on the frequency and modal mass of the bar as well as the mass and damping coefficient of the TMD. Maximum chatter stability is then obtained by tuning the damper to a frequency that minimizes the negative real part of the frequency response function [2]. This task is quite straightforward for smaller tools in rigid clamping because the frequency of the cutting tool will be close to the natural frequency found by ideal clamping by FEM simulation. The problem arises when the tool is mounted in a weak clamping because in this case the measured natural frequency can be considerably lower than the ideal natural frequency found by FEM. A simple but naive way to account for this is to assume that the frequency change is caused by a stiffness loss in the clamping and introduce a stiffness ratio, SR, in the design given by:

$$SR = \frac{k_{actual}}{k_{FEM}} = \frac{f_{actual}^2}{f_{FEM}^2} \quad (1)$$

Where  $k_{actual}$  and  $f_{actual}$  refers to stiffness and natural frequency from experimental measurements on the tool mounted in the machine. And  $k_{FEM}$  and  $f_{FEM}$  refers to the stiffness and natural frequency predicted by FE-modeling of the cutting tool with fixed support.

Finding SR for the design usually involves both a significant amount of experience and some qualified guessing. Small tools in stiff machines leads to SR close to 1, while large tools in weak machines can have SR less than 0.5.

Another possibility is to completely model the modes of the machine-tool and the cutting-tool and find the actual frequency of the first bending mode. This requires an accurate model of the machine-tool which is not often available. An alternative approach is to use substructuring techniques to couple models of the cutting tool and the machine tool together. However, substructuring of continuous systems requires information about the rotational degrees of freedom which are not easily acquired by experimental techniques as shown in e.g. [3]. Another approach suggested by Park et al., [4], is to combine numerical models of the cutting tool with experimental measurements of the machine tool to estimate the rotational degrees of freedom in the coupling nodes and perform substructuring using receptance coupling techniques, [5]. The substructuring approach will require a substantial amount of measurements of high accuracy to be successfully applied to this specific problem. Therefore, a need for a faster, more simplistic, approach to obtain a prediction of the resonance frequency of the cutting tool in this specific application is of interest within the industry.

The purpose of this paper is to develop a simplified dynamic model that considers only the most prominent coupled modes, and to show by experiment that the frequency behavior of the system can be adequately explained.

## 2. Model development

We will keep the parameter SR as a measure of the deviation of the modeled system from the ideal rigid clamping, but we abandon the idea that the SR is a static characteristic of the weak clamping alone. Instead we will look at the tool body and clamping unit as a dynamic system with two degrees-of-freedom (DOF). We will use our Giana Lathe as a test bench, and we will focus on lateral vibrations since these are in the most critical (radial) direction of the cutting process.

### 2.1. Initial modal measurements

To get an idea of how to build our model we mount a large tool body in our Giana lathe and do a “roving hammer” frequency response function (FRF) measurement. Here an accelerometer is placed at the front of the tool while the FRF is recorded by hitting with the hammer in several positions along the z-axis of the tool and clamping shown in Fig 3.

Fig. 1 shows the FRF of a 3200mm long tool body with a diameter of 200mm, clamped at an overhang of 1521mm. Two distinct resonance peaks are present at 63 and 105 Hz.

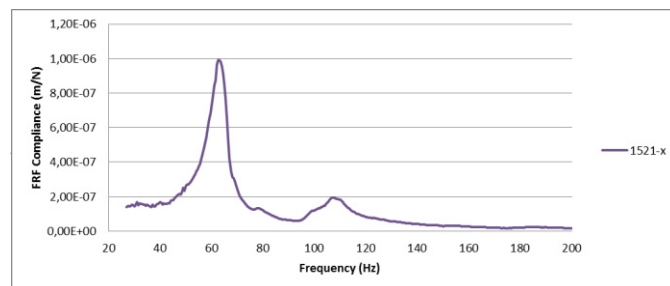


Fig. 1. Imaginary part of an impulse hammer FRF measurement showing two resonance peaks.

Fig. 2 shows the corresponding mode shapes found by modal analysis of FRF measurements in 8 positions along the cutting tool, where  $z=0$  corresponds to the front of the clamping structure while the tip of the tool is at 1.52 m. The two curves are found by plotting the peak values of the imaginary part of the FRF at the two resonance frequencies 63 Hz and 105 Hz. The curves pass through zero at a point close to the position of the x-axis lead screw of the tool holder. These mode shapes indicate that the modes we see are a superposition of a bending mode of the bar and a rotational rigid body mode of the clamping unit. Thus, in the following, we restrict our model to these two degrees of freedom.

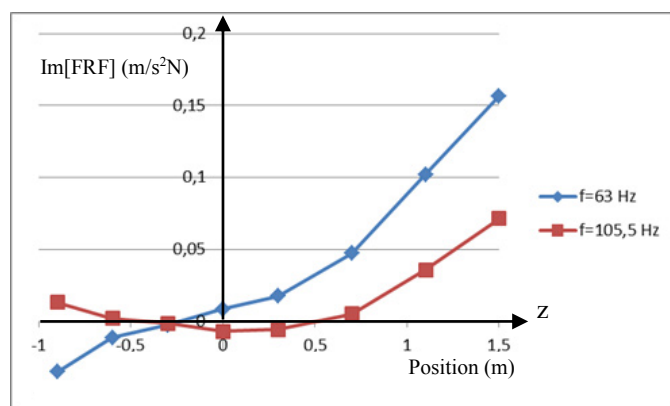


Fig. 2. Mode shapes found by plotting the peak values of the imaginary part of the FRF as a function of measurement position.

### 2.2. Theory

The first DOF is the first bending mode of the tool body, ideally clamped in an infinitely rigid tool holder as shown in Fig. 3. This is the fundamental mode of our FEM model, for which we know both stiffness,  $k_1$ , and eigenfrequency,  $f_1$ . From these we can calculate the equivalent modal mass,  $m_1$ , and model this mode as a mass-spring-damper system, with a small damping,  $c_1$ , due to material loss. The frequency of this DOF is given by:

$$f_1 = \frac{1}{2\pi} \sqrt{\frac{k_1}{m_1}} \quad (2)$$

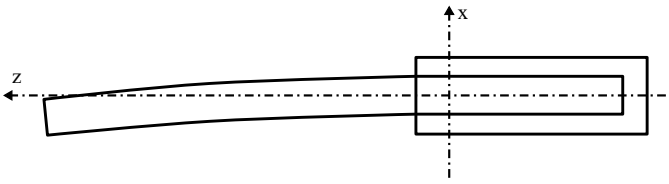


Fig. 3. First DOF - bending mode of the boring bar.

The second DOF is a rotational mode of the tool and clamping unit as shown in Fig. 4. This mode is modelled as a rigid body with a moment of inertia,  $J_{TOT}$ , determined by the tool plus the clamping unit rotating around a point close to the x-axis lead screw of the tool holder. A rotational spring,  $k_r$ , is used to model the restoring force, and a moderate damping,  $c_r$ , is also present due to friction in the lead screw and the guide rails. The frequency of this DOF is given by:

$$f_r = \frac{1}{2\pi} \sqrt{\frac{k_r}{J_{TOT}}} \quad (3)$$

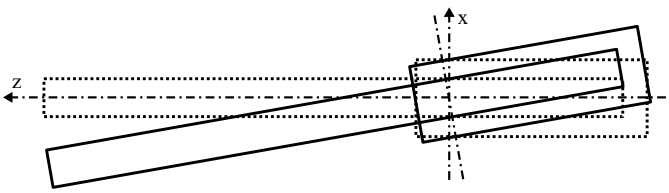


Fig. 4. Second DOF – angular rotation of the tool and clamping unit.

We now combine the rotational mode with the bending mode into the simplified model shown in Fig. 5. The bending of the bar, due to external forces, or inertial forces from the mass  $m_1$ , corresponds to an elongation of the spring  $x_1-x_0$ .

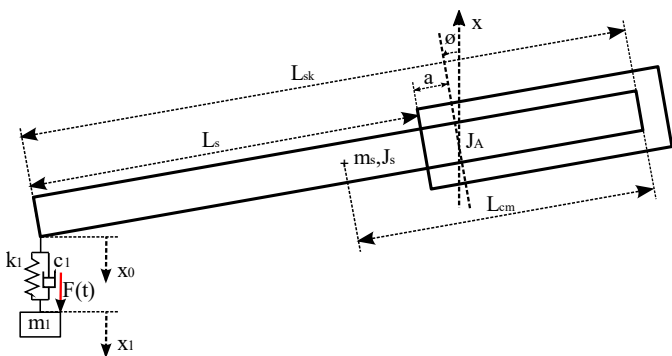


Fig. 5. The tool body with its first bending mode modeled as a mass-spring-damper (mkc) coupled with a rotational stiff body mode.

$J_a$  is the moment of inertia of the tool holder relative the center of rotation,  $J_s$  is the moment of inertia of the tool relative its mass center, and  $m_s$  is the mass of the tool. The position of the tool tip is given by the superposition of bending and rotation which corresponds to the position  $x_1$ , of the mass  $m_1$  in the figure. With only two DOFs it is straightforward to state the

differential equations for the system and find the frequency response. The two second order coupled mode equations can be written as:

$$\begin{aligned} m_1 \ddot{x}_1 &= -c_1 \dot{x}_1 - k_1 x_1 + k_1 r \theta + c_1 r \dot{\theta} + F(t) \\ J_{tot} \ddot{\theta} &= -(r^2 c_1 + c_r) \dot{\theta} - (r^2 k_1 + k_r) \theta + r c_1 \dot{x}_1 + r k_1 x_1 \end{aligned} \quad (4)$$

In Eq. (4) we have assumed small angular deviations meaning that  $x_0 \approx r\theta$ , where  $r=L_s+a$ , is the distance from tool tip to the point of rotation as indicated in Fig. 5. The total moment of inertia,  $J_{TOT}$ , depends on the distance from the center of mass to the point of rotation, and is given by:

$$J_{tot} = J_a + J_s + m_s (L_{cm} - (L_{sk} - L_s - a))^2 \quad (5)$$

From Eq. (4) we can find the eigenfrequencies,  $f_a$  and  $f_b$  of the coupled undamped ( $c_1=c_r=0$ ) system. We express these as a function of the two natural frequencies  $f_l$  and  $f_r$  from Eq. (2) and Eq. (3):

$$f_{a,b}^2 = \frac{1}{2} \left[ f_l^2 (1 + \mu_r) + f_r^2 \pm \sqrt{(f_l^2 (1 + \mu_r) + f_r^2)^2 - 4 f_l^2 f_r^2} \right] \quad (6)$$

Here  $f_a$  is the lowest frequency corresponding to the minus sign in Eq. (6). The amount of coupling between the modes is determined by,  $\mu_r$ , corresponding to a ratio of two moments of inertia:

$$\mu_r = \frac{r^2 m_1}{J_{TOT}} \quad (7)$$

Fig. 6 shows how the two modal frequencies  $f_a$  and  $f_b$  depend on  $f_l$ ,  $f_r$  and  $\mu_r$ . The mutual interaction between the modes, tend to push the modal frequencies away from each other. The interaction is largest when  $f_l$  equals  $f_r$ , and  $\mu_r$  is large.

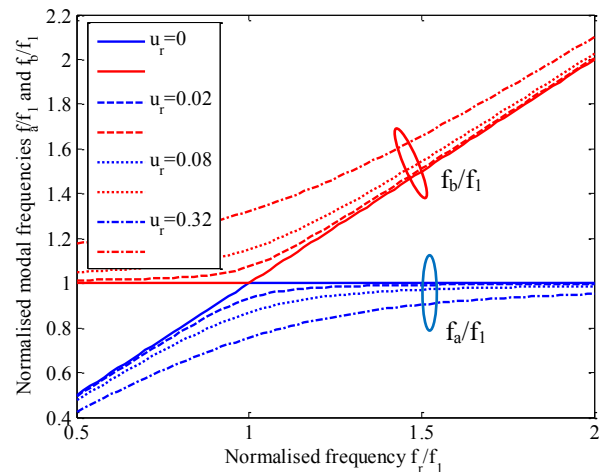


Fig. 6. Eigenfrequencies of the coupled modes as a function of frequency ratio  $f_r/f_1$ , and the moment of inertia ratio,  $\mu_r$ , of the two uncoupled modes.

The lowest frequency,  $f_a$ , is the critical frequency we are looking for, and an equivalent “dynamic stiffness ratio”, DSR, can be found by dividing Eq. (6). by the square of the natural frequency of the pure bending mode,  $f_r^2$ . If we also introduce the normalised frequency ratio,  $q=f_r/f_1$ , between the rotational mode and the bending mode, we find:

$$DSR = \frac{1}{2} \left[ 1 + \mu_r + q^2 - \sqrt{(1 + \mu_r + q^2)^2 - 4q^2} \right] \quad (8)$$

We note that the term “stiffness ratio” is somewhat misleading but we choose to keep it as a measure of the quality of the clamping that we can relate to earlier work. Fig. 7 shows DSR as a function of the normalised frequency,  $q$ , and the inertial ratio,  $\mu_r$ . We have assumed that the natural frequency of the tool holder is higher than the bending frequency of the tool itself,  $f_r > f_1$ , which is usually the case for large slender tools.

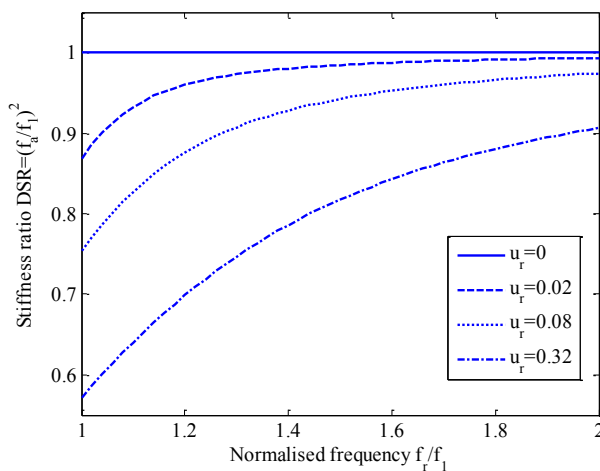


Fig. 7. Dynamic stiffness ratio as a function of frequency ratio  $f_r/f_1$ , and the moment of inertia ratio,  $\mu_r$ , of the two uncoupled modes.

From Fig. 7 we see, as expected, that increasing  $\mu_r$ , reduces the frequency  $f_a$ , leading to a lower DSR. We note especially the strong dependence on the ratio between the bending frequency and the rotational frequency. As they approach each other, the DSR drops rapidly.

### 2.3. Experiment

To test our model, we mount the tool body (without damper inside) in our Giana test lathe and clamp it at different overhang lengths. From ANSYS FE-software, we get the following parameters for the bar:

Table 1. FEM parameters for the tool body ideally clamped at two different overhang lengths.

Diameter	Ø	200	mm
Length	Lsk	3200	mm
Mass	ms	474	Kg
Center of mass	Lcm	1250	mm
Moment of inertia	Js	334	kg·m <sup>2</sup>

Overhang	$L_s$	2118	1521	mm
Modal frequency	$f_1$	45	89	Hz
Static stiffness	$k_1$	$4.2 \cdot 10^6$	$11 \cdot 10^6$	N/m
Modal mass	$m_1$	52	36	Kg

Fig. 8 shows the measured FRFs in both horizontal and vertical direction for three different overhang lengths 2118 mm, 1916 mm and 1521 mm. Comparing the ANSYS frequencies from table 1 with the measured response we find as expected that the measured frequencies are lower and that the relative difference is largest for the shortest overhang. At 1521 mm we should have a resonance at 89 Hz if the clamping was ideal, but we measure 63 Hz, corresponding to SR=0.5.

Note the large damping of the 2118-x measurement in Fig. 8. A large loss at a specific resonance frequency is typical for complex machines where loss can occur at specific excitations. Ignoring this anomaly does not affect the results.

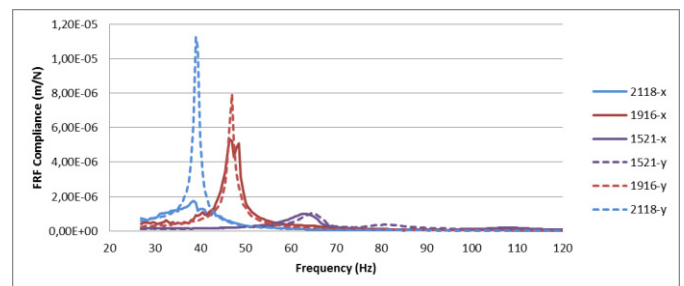


Fig 8. FRF measurements for the tool body, measured in horizontal, (x), and vertical, (y), direction at three overhang lengths (1521mm, 1916mm and 2118mm).

If we compare the 1521-x measurement in Fig. 2 with the measurements at longer overhangs in Fig. 8, we find that the higher frequency mode becomes less pronounced at longer overhangs.

This behavior becomes clear when we insert the ANSYS results for the bending modes of the ideally clamped tool body into Eq. (4) and from this simulate and plot the magnitude of the FRF. But first we must find some parameters for the clamping unit. The peak at 110 Hz in Fig. 2, makes us guess that the frequency  $f_r$ , of the rotational mode is close to this. The low DSR-value that we measure for the shortest overhang, tells us that the moments of inertia ratio,  $\mu_r$ , cannot be very small. By trying  $J_A=300 \text{ kgm}^2$ ,  $f_r=107 \text{ Hz}$  and  $\mu_r=0.05$ , we get the simulated FRFs shown in Fig. 9. In the simulation we have varied the overhang from 1521 mm to 2118 mm in 5 steps. The curves have been offset slightly to increase the visibility. The general behavior fits well with what we observe in our measurements in Fig. 8 and Fig. 2.

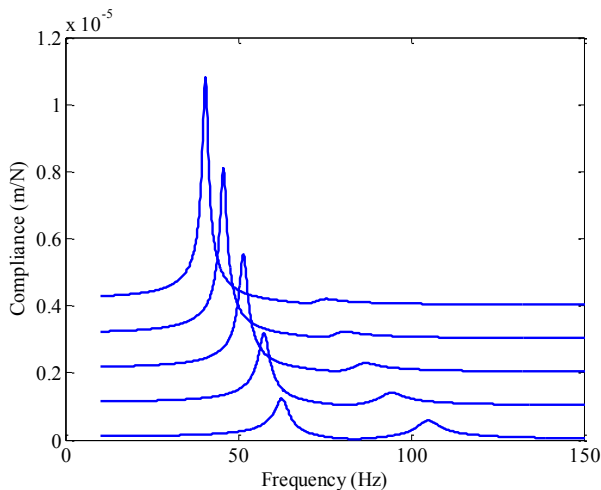


Fig. 9. Simulated FRF curves for the tool body clamped at 5 different overhang lengths from 1521mm to 2118mm. The curves have been offset to increase visibility. The uppermost curve corresponds to the longest overhang.

The two peaks in the simulated responses in Fig. 9 correspond to our coupled modes with frequencies  $f_a$  and  $f_b$ . Of these, it is the lowest frequency  $f_a$  that is critical with respect to tool stability.

Fig. 10 shows a plot of this frequency, which is based on our model ( $f_a$ , solid line), together with the FEM frequency ( $f_i$ , dashed line) corresponding to ideal, rigid, clamping conditions, and the actual frequencies (circles) found from the FRF measurements in Fig. 8. It should be noted that the FEM frequency corresponds to the bending mode in Fig. 3, while our model includes also the rotation of the tool and clamping unit, which in this case is necessary to describe the frequency behavior correctly. From Fig. 10 it is clear, that the deviation from ideal clamping changes with the tool overhang in a way that we can predict if we know the characteristics of the tool and clamping unit. The fact that the deviation is larger for the short overhang than it is for the long, is explained by the increased coupling that occurs when the bending frequency of the tool,  $f_i$ , approaches the rotational frequency of the tool and clamping unit,  $f_r$ , as shown in Fig. 7.

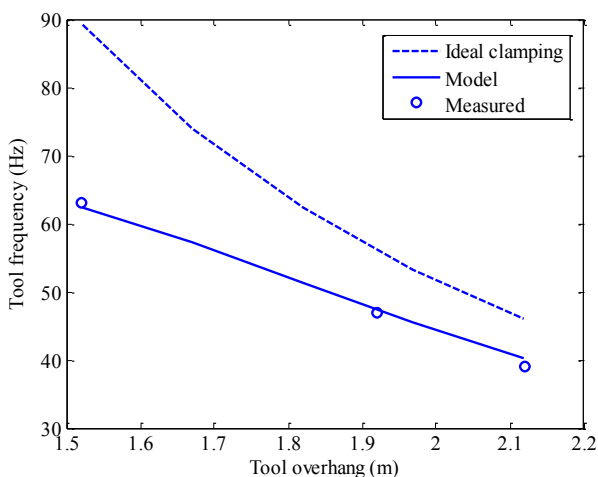


Fig. 10. Comparison of measured tool frequencies with frequencies from the 2-DOF model and from ideal rigid clamping in ANSYS.

### 3. Conclusions

A simplified approach to capture and model the change in dynamics caused by the clamping of a big boring bar into a machine tools has been presented. The modeling approach described capture, quite accurately, the behavior of the boring bar and explains why and how the stiffness ratio varies with overhang length. This type of model can be a useful tool for predicting the critical frequency that a certain tool body will have in a specific machine. The measured stiffness ratio is not only dependent on the machine clamping stiffness, but on the length, frequency and mass of the tool as well as stiffness and moment of inertia of the clamping unit. The next step will be to develop a method to characterize the clamping unit separately by modelling and/or measuring to provide better estimates of the dynamics in the machine-tool/tool-holder.

### 4. References

- [1] E. I. Rivin and H. Kang, "Enhancement of dynamic stability of cantilever tooling structures," *International Journal of Machine Tools and Manufacture*, vol. 32, pp. 539-561, 1992.
- [2] N. D. Sims, "Vibration absorbers for chatter suppression: A new analytical tuning methodology," *Journal of Sound and Vibration*, vol. 301, pp. 592-607, 2007.
- [3] A. Liljehrn, *Machine tool dynamics : a constrained state-space substructuring approach.*, Göteborg : Chalmers University of Technology, 2016., 2016.
- [4] S. S. Park, Y. Altintas and M. Movahhedy, "Receptance coupling for end mills," *International Journal of Machine Tools and Manufacture*, vol. 43, pp. 889-896, 2003.
- [5] B. Jetmundsen, R. L. Bielawa and W. G. Flannelly, "Generalized Frequency Domain Substructure Synthesis," *Journal of the American Helicopter Society*, vol. 33, pp. 55-64, 1988.